AJNR

Radiation Necrosis Versus Glioma Recurrence: Conventional MR Imaging Clues to Diagnosis

Mark E. Mullins, Glenn D. Barest, Pamela W. Schaefer, Fred H. Hochberg, R. Gilberto Gonzalez and Michael H. Lev

Radiation Necrosis Versus Glioma Recurrence: Conventional MR Imaging Clues to Diagnosis

Mark E. Mullins, Glenn D. Barest, Pamela W. Schaefer, Fred H. Hochberg,
R. Gilberto Gonzalez, and Michael H. Lev

BACKGROUND AND PURPOSE: Conventional MR imaging findings are considered to be inadequate for reliably distinguishing radiation necrosis from tumor recurrence in patients with glioma. Despite this belief, we hypothesized that certain conventional MR imaging findings, alone or in combination, though not definitive, may favor one or another of these diagnoses in proton beam–treated patients with new enhancing lesions on serial scanning.

METHODS: MR imaging findings (axial T1-, T2-, and post-gadolinium T1-weighted) of 27 proton beam radiation therapy patients with high-grade gliomas were retrospectively reviewed. Entry criteria included new MR imaging enhancing lesions after treatment and histologically unequivocal biopsy proof of diagnosis. Readers rated corpus callosum involvement, midline spread, subependymal spread, new discrete multiple enhancing foci, a "spreading wavefront" appearance, and septum pellucidum involvement. Statistical analysis was by the Fisher exact test.

RESULTS: Corpus callosum involvement in combination with multiple other findings was highly associated with progressive glioma. These combinations included involvement of the corpus callosum with multiple enhancing foci ($P = .02$), involvement of the corpus callosum with crossing the midline and multiple enhancing lesions ($P = .04$), and involvement of the corpus callosum with subependymal spread and multiple enhancing lesions ($P = .01$).

CONCLUSIONS: In proton beam–treated patients with glioma, corpus callosum involvement, in conjunction with multiple enhancing lesions with or without crossing of the midline and subependymal spread, favors predominant glioma progression. Overall, combinations of enhancement patterns were more likely than individual patterns to distinguish necrosis from predominant tumor progression. Together with clinical and functional imaging findings, these results may assist in determining the need for biopsy.

The distinction between radiation necrosis and recurrent high-grade glioma remains a challenge despite advanced imaging techniques such as perfusion- and diffusion-weighted MR imaging (1–5), MR spectroscopy (6), and positron emission tomography (7–9). MR imaging characteristics of high-grade tumor classically include intravenous contrast enhancement, mass effect, and associated vasogenic edema (10). Unfortunately, radiation necrosis entails the same

core list of characteristics on conventional MR imaging. Kumar et al (11) recently discussed guidelines based on their experience that favor radiation necrosis over recurrent and/or progressive high-grade tumor in presentation: 1, conversion from no enhancement to enhancement; 2, remote new enhancement; 3, new periventricular enhancement, and 4, soap-bubble or Swiss cheese enhancement.

In this study, we report our experience with high-grade gliomas that have undergone proton beam radiation therapy and have developed new abnormal enhancement on follow-up imaging. The differential diagnosis for these patients was between predominantly recurrent tumor versus predominantly radiation necrosis (allowing for the fact that at least microscopic glioma is almost certainly present to some degree in all such patients, despite prior treatment). Conventional MR imaging characteristics of these lesions were independently rated and statistically analyzed, compared with an unequivocal histologic or clinical gold standard. We hypothesized that some conventional MR imaging findings, alone or in com-

TABLE 1: Individual MR imaging signs of tumor recurrence versus radiation necrosis results

	Corpus Callosum	Midline Spread	Subependymal Spread	Multiple Lesions	Spreading Wavefront	Septum Pellucidum	Pathologic Diagnosis
Totals							
Presence	4	1	6	3	6	4	Necrosis
Absence	8	11	6	9	6	8	Necrosis
Presence	10	2	11	9	3	2	Tumor
Absence	5	13	4	6	12	13	Tumor
P value*	.12	1	.26	.12	.13	.36	
Sign favors diagnosis of:	Tumor	Neither	Tumor	Tumor	Necrosis	Necrosis	
Sensitivity (%)	66.7	N/A	73.3	60	50	33.3	
Specificity (%)	66.7	N/A	50	75	81.3	86.7	
Positive predictive value (%)	71.4	N/A	64.7	75	66.7	66.7	
Negative predictive value (%)	61.5	N/A	60	60	68.4	61.9	
Accuracy (%)	66.7	N/A	63	67	68	63	

* Fisher's exact 2-tailed test.

bination, though not definitive, may favor tumor recurrence or radiation necrosis in proton beam–treated patients with new enhancing lesions on serial scanning. Our premise was to identify conventional MR enhancement patterns in post–proton beam–treated patients with glioma, which favor either predominantly tumor recurrence or predominantly radiation necrosis. Our goal was not to obviate advanced imaging or biopsy but rather to extract as much data as possible from the conventional MR imaging, so as to better determine the need for these additional studies.

Methods

Patient Enrollment

During a 17-month period, 27 consecutive patients who had received proton beam radiation therapy as a primary treatment technique for biopsy-proven high-grade intracranial intraparenchymal gliomas and who had possible recurrent glioma versus radiation necrosis on standard follow-up imaging (new abnormally enhancing tissue) were enrolled in the study. Patient symptoms were not an inclusion criterion. Patient chemotherapy was not an inclusion criterion and was variable across the group; many of the patients were enrolled in studies of experimental chemotherapeutics. All patients received fractionated photon radiation therapy in addition to proton beam radiation therapy, but doses or proton beam radiation therapy and photon therapy were not standardized across the patient group. Radiation dose ranges were typical for patients both outside of this group at our hospital and in the literature (12, 13). All cases were identified within a time period in which radiation necrosis was a viable clinical possibility to account for the new findings; specifically, scans were performed at more than 6 months following radiation treatment. Patients without a pathology-proven diagnosis on subsequent brain biopsy were excluded.

MR Imaging

MR imaging was performed on a 1.5-T whole-body scanner with an echoplanar retrofit. T1-weighted sagittal images were acquired with TR/TE, 650/16; field of view of 20 cm; an acquisition matrix of 256 × 192 pixels; section thickness of 5 mm with a 1-mm gap; and 1 signal-intensity average. Fluid-attenuated inversion recovery axial MR images were obtained with TR/TE/TI, 10,002/141/2200; field of view of 24 cm; acquisition matrix of 256 × 192 pixels; section thickness of 5 mm with a 1-mm gap; and 1 signal-intensity average. Fast spin-echo T2-weighted MR axial images were obtained with TR/TE, 4200/102; field of view of 20 cm; acquisition matrix of 256 × 256 pixels; section thickness of 5 mm with a 1-mm gap; and 1 signal-intensity average. Postcontrast (gadopentate) material T1-weighted triplanar images were obtained using parameters as described previously for the precontrast material T1-weighted images.

Data Interpretation

Images were initially reviewed in a blinded fashion by 2 of 4 randomized neuroradiologists. The following MR findings were evaluated as positive or negative: 1, involvement of the corpus callosum; 2, spread across the midline; 3, subependymal spread; 4, involvement of the septum pellucidum; 5, multiple discrete new-enhancing foci; and 6, a "spreading-wavefront" pattern of enhancement (meaning that the margins of the enhancement were ill-defined, as opposed to well-defined). In cases in which the 2 blinded observations agreed, the result was accepted outright. In cases in which there was disagreement, a consensus of the group was achieved.

Pathology Follow-up

New-enhancing lesions were excised totally or biopsied for definitive characterization based on neurosurgical clinical evaluation of resectability. In cases of biopsy without total resection, the most clinically suspicious enhancing nodular lesion portion was sampled. The decision for biopsy site localization was ultimately defined by the neurosurgeon, guided by neuroradiology, neurology, and neurooncology input. The final primary pathology diagnosis was used for statistical comparisons. Lesions with tumor or mixed tumor and necrosis with predominant viable tumor were treated as "tumor" for statistical comparisons because both would be treated clinically as predominantly recurrent tumor for the purposes of subsequent treatment.

Statistical Analysis

Consensus results were tabulated for both readers and used for statistical evaluations of both individual signs and combinations of 2 and 3 signs in the cohort. Standard statistical analysis was performed using the Fisher exact 2-tailed tests (www.graphpad.com/quickcalcs). $P < .05$ was considered statistically significant.

Human Research Committee Approval

The Human Research Committee of our hospital approved this study.

TABLE 2: Combination of two MR imaging signs of tumor recurrence versus radiation necrosis results

	CC MID	CC SUB	CC MEF	CC SPW	CC SEP	MID SUB	MID MEF	MID SPW	MID SEP	SUB MEF	SUB SPW	SUB SEP	MEF SPW	MEF SEP	SPW SEP	Pathologic Diagnosis
Presence	5	10	7	10	8	7	4	7	5	9	12	10	9	7	10	Necrosis
Absence	19	14	17	14	16	17	20	17	19	15	12	14	15	17	14	Necrosis
Presence	12	21	19	13	12	13	11	5	4	20	14	13	12	11	5	Tumor
Absence	18	9	11	17	18	17	19	25	26	10	16	17	18	19	25	Tumor
P value*	.15	.05	.02	1	.78	.4	.13	.33	.48	.05	1	1	1	.77	.07	
Sign favors diagnosis of:	Tumor	Tumor	Tumor	Neither	Tumor	Tumor	Tumor	Neither	Neither	Tumor	Neither	Neither	Tumor	Tumor	Necrosis	
Se (%)	40.0	70	63.3	N/A	40	43	36.7	N/A	N/A	66.7	N/A	N/A	40	36.7	41.7	
Sp (%)	79.2	58.3	70.8	N/A	66.7	70.8	83.3	N/A	N/A	62.5	N/A	N/A	62.5	70.8	83.3	
PPV (%)	70.6	67.7	73.1	N/A	60	65	73.3	N/A	N/A	69	N/A	N/A	57.1	61.1	66.7	
NPV (%)	51.4	60.9	60.7	N/A	47.1	50	51.3	N/A	N/A	60	N/A	N/A	45.5	47.2	64.1	
Accuracy	57.4	64.8	66.7	N/A	51.9	55.6	57.4	N/A	N/A	64.8	N/A	N/A	50	51.9	64.8	

CC indicates corpus callosum involvement; MID, midline spread; SUB, subependymal spread; MEF, new discrete multiple enhancing foci; SPW, "spreading wavefront" appearance; SEP, septum pellucidum involvement; Se, sensitivity; Sp, specificity; PPV, positive predictive values; and NPV, negative predictive values.

* Fisher's exact 2-tailed test.

Results

Twenty-seven consecutive patients were enrolled after exclusion criteria were applied. Based upon Daumas-Duport pathologic classification, 4 patients had grade II/IV astrocytoma, 7 had grade III/IV, 4 had grade III-IV/IV, and 12 had grade IV/IV. All tumors enhanced before surgery and treatment.

Fifteen patients had predominant recurrent tumor based on biopsy results, whereas 12 had predominant radiation necrosis. Disagreement between observers never varied by more than 1 point in the grading system and never changed the category assignment (data not shown).

Results for the MR imaging findings evaluated are listed in Table 1. The following assessments represent the predominant pathologic diagnosis for the new enhancing lesion: A spreading wavefront pattern was present in 3 of 15 recurrent tumors and 6 of 12 necrosis cases ($P = .13$). Septum pellucidum involvement occurred in 2/15 recurrent gliomas and 4/12 necrosis cases ($P = .36$). Multiple new-enhancing foci were present in 9/15 recurrences and 3/12 necrosis cases ($P = .12$). Involvement of the corpus callosum was present in 10/15 recurrences and 4/12 necrosis cases ($P = .12$). The midline was crossed in 2/15 recurrences and 1/12 necrosis cases ($P = 1$). Subependymal spread was present in 11/15 recurrences and 6/12 necrosis cases ($P = .26$). None of the individual signs were statistically significant.

Results for combinations of 2 MR imaging signs are listed in Table 2. The following assessments represent the predominant pathologic diagnosis for the new enhancing lesion. Involvement of the corpus callosum with multiple enhancing foci was statistically significant ($P = .02$), favoring predominant tumor recurrence. The remainder of the combination of 2 MR imaging findings was not statistically significant.

Results for combinations of 3 MR imaging signs are listed in Table 3. The following assessments represent the predominant pathologic diagnosis for the new enhancing lesion. Involvement of the corpus callosum with crossing of the midline and multiple enhancing lesions was statistically significant ($P = .04$), favoring tumor recurrence. Involvement of the corpus callosum with subependymal spread and multiple enhancing lesions was statistically significant ($P = .01$), favoring tumor recurrence. The remainder of the combination of 3 MR imaging findings was not statistically significant.

Discussion

Radiation necrosis following radiation therapy for brain tumor is not uncommon (5%–24% overall) and has been well described in imaging and autopsy studies (14, 15). The high frequency of this treatment effect, together with similar conventional imaging characteristics of gliomas, including contrast enhancement, mass effect, and vasogenic edema, has confounded differential diagnostic evaluation. Some prior studies have suggested possible further characterization based on conventional imaging findings

TABLE 3: Combination of two MR imaging signs of tumor recurrence versus radiation necrosis results

	CC MID SUB	CC MID MEF	CC MID SPW	CC MID SEP	CC SUB MEF	CC SUB SPW	CC SUB SEP	CC MEF SPW	CC MEF SEP	CC SPW SEP	Pathologic Diagnosis
Presence	11	8	11	9	13	16	14	13	11	14	Necrosis
Absence	25	28	25	27	23	20	22	23	25	22	Necrosis
Presence	23	21	15	14	30	24	23	22	21	15	Tumor
Absence	22	24	30	31	15	21	22	23	24	30	Tumor
P value*	.07	.04	.81	.62	.01	.50	.37	.27	.17	.64	
Sign favors diagnosis of	Tumor	Tumor	Tumor	Tumor	Tumor	Tumor	Tumor	Tumor	Tumor	Neither	
Se (%)	51.1	46.7	33.3	31.1	66.7	53.3	51.1	48.9	46.7	N/A	
Sp (%)	69.4	77.8	69.4	75.0	63.9	55.6	61.1	63.9	69.4	N/A	
PPV (%)	67.6	72.4	57.7	60.9	69.8	60.0	62.2	62.9	65.6	N/A	
NPV (%)	53.2	53.8	45.5	46.6	60.5	48.8	50.0	50.0	51.0	N/A	
Accuracy (%)	59.3	60.5	49.4	50.6	65.4	54.3	55.6	55.6	56.8	N/A	

CC indicates corpus callosum involvement; MID, midline spread; SUB, subependymal spread; MEF, new discrete multiple enhancing foci; SPW, "spreading wavefront" appearance; SEP, septum pellucidum involvement; Se, sensitivity; Sp, specficity; PPV, positive predictive values; and NPV, negative predictive values.

* Fisher's exact 2-tailed test.

(11). Use of advanced techniques including MR perfusion, diffusion-weighted imaging, and positron emission tomography has suggested increased sensitivity and accuracy compared with conventional MR imaging, but it would be useful to glean as much information from conventional MR imaging as possible, given that not all imaging centers apply these advanced diagnostic techniques and that routine follow-up imaging most typically entails only noncontrast- combined with postcontrast-enhanced images. Given this motivation and the results of previous investigations, we reviewed our experience with conventional MR imaging in this population. Our results suggest several trends (Tables 1–3).

Our results concerning individual features, including spreading wavefront (Figs 1 and 2), midline spread (Figs 3 and 4), new involvement of the corpus callosum (Fig 4), and subependymal spread (Fig 4) did not reach statistical significance. It is unclear why these previously expected conventional MR imaging characteristics did not yield statistical results when evaluated individually. Indeed, lack of demonstration of meaningful involvement of the corpus callosum and subependymal spaces is curious given the results of Kumar et al (11); however, that study addressed observation of these signs in both groups rather than differentiation.

Combinations of MR imaging findings yielded several statistically significant results and suggest that combinations of findings on MR imaging are likely more useful than individual signs. Several statistically significant combinations favored recurrent tumor: involvement of the corpus callosum with subependymal spread, involvement of the corpus callosum with crossing of the midline and multiple lesions, and involvement of the corpus callosum with subependymal spread and multiple lesions. Additional combinations of findings favoring tumor recurrence were also observed but did not meet statistical significance, and are thus of unproven clinical value.

Despite statistically significant P values within some of the combinations, the remaining statistical parameters were suboptimal. Specifically, sensitivity, specificity, negative and positive predictive value, and accuracies were uniformly less than 78% in these combination groups. The reason for these observations is unclear but may be due to the heterogeneity of the groups. Furthermore, the clinical applicability and generalizability of these observations are thus indefinite. Thus, further study using more homogeneous patient, tumor type, and treatment groups is indicated. Nevertheless, these find-
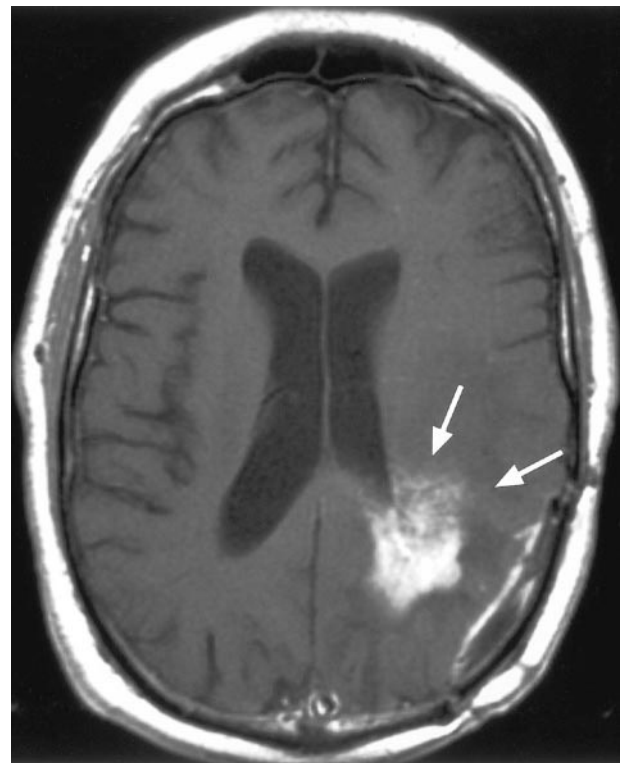

FIG 1.   60-year-old woman with a history of left parietal anaplastic astrocytoma and new abnormal enhancement on follow-up imaging after surgery and proton beam irradiation therapy. Arrows on this postcontrast axial T1-weighted image illustrate the "spreading wavefront" appearance. Biopsy of this lesion yielded radiation necrosis.
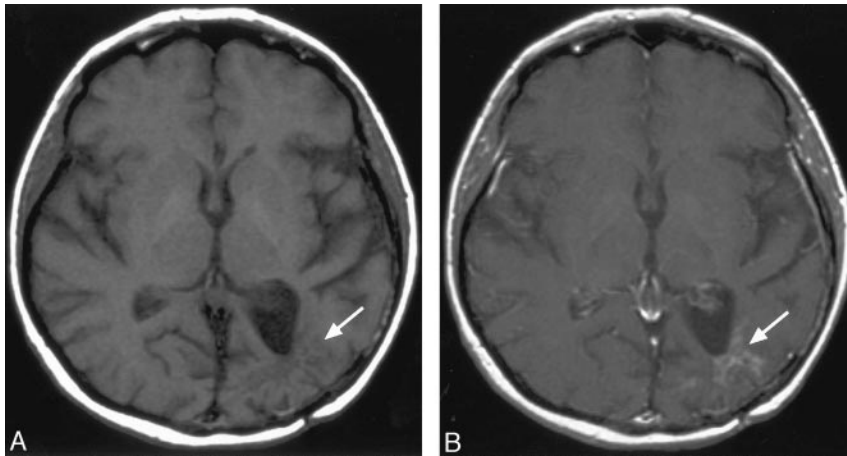
FIG 2. 50-year-old woman with history of left parieto-temporo-occipital glioblastoma multiforme and new abnormal enhancement on follow-up imaging after surgery and proton beam irradiation therapy. *A,* Arrows on this precontrast axial T1-weighted image illustrate the location of abnormal enhancement. *B,* Arrows on this postcontrast axial T1-weighted image illustrate the spreading wavefront appearance along one of the dominant borders of the lesion; subependymal involvement that extended up to involve the corpus callosum is also observed. Biopsy of a portion of the abnormality yielded recurrent tumor.
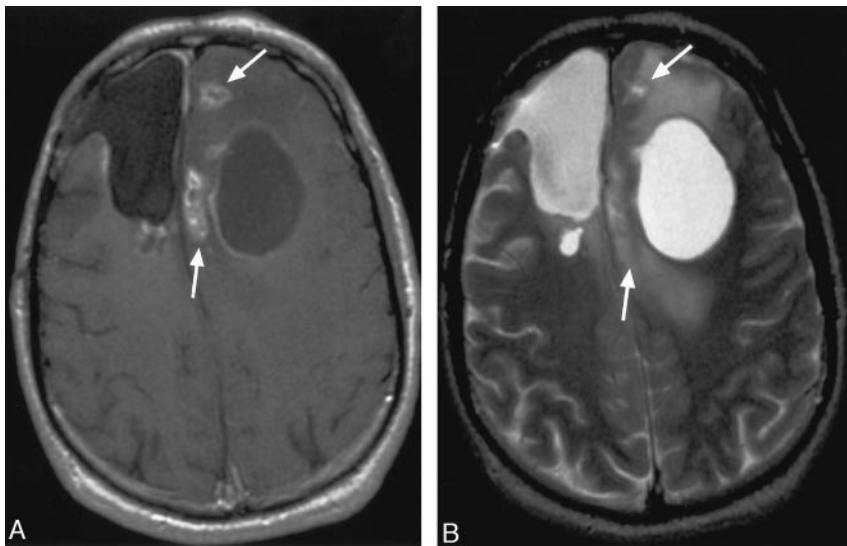

FIG 3. 57-year-old woman with history of right frontal glioblastoma multiforme and new abnormal enhancement on follow-up imaging after surgery and proton beam irradiation therapy. *A,* Arrows on this post-contrast axial T1-weighted image illustrate multiple enhancing lesions and spread to the contralateral hemisphere. *B,* Arrows on this postcontrast axial T2-weighted image illustrate the location of abnormal enhancement on the axial T1-weighted images, as well as associated vasogenic or tumor edema. Biopsy of a portion of the abnormality yielded recurrent tumor.

ings may still be of clinical assistance, based upon their statistically significant *P* values.

Correlation with functional imaging examinations such as MR spectroscopy, tumor perfusion imaging, and positron imaging tomography would have been useful in all patients within this group. However, not all of these examinations were performed in all patients. Moreover, during the timeframe when this examination was performed, these techniques were not readily or universally available. Thus, further study to compare and contrast these methodologies is indicated.

A primary limitation of our study is that it is expected that patients with high-grade gliomas will have residual tumor despite even the most careful surgical resection and treatment; thus, we have aimed to identify what the primary cause of a new-enhancing lesion represents. It is certain that these sites will contain at least some tumor, but subsequent treatment will change depending on whether the predominant pathology at this location is progressive tumor or radiation necrosis. It is in this light that we have sought to answer this complex but focused question.

Our study has other limitations that may also hinder its generalizability, including its retrospective design, relatively small sample size, heterogeneity of

tumor type, chemotherapy, and photon radiation treatment. Our findings do indeed represent a "snapshot" in time and thus represent only a portion of the patient's data. These findings could have potentially contributed to both selection and assignment biases. Results were based on pathology obtained by selective neurosurgical biopsy in some instances rather than total lesion resection, and thus the choice of biopsy location and variations in pathology interpretation and/or reporting could have potentially biased the results. For example, some lesions may in fact be composed of predominantly mixed tumor more than radiation necrosis, whereas the biopsy yielded predominantly radiation necrosis.

These limitations are based on clinical limitations (eg, wide margins and total excision cannot be obtained in these human patients unless clinically indicated), and our study, data, and interpretations are based on the best information available to us. It is also not clear whether the results would be applicable to nonproton beam–only irradiated fields; thus further study to evaluate these parameters in association with other forms of radiation treatment including photon beam is indicated. Statistical evaluation of these parameters, including combinatorial evaluations, may also oversimplify the
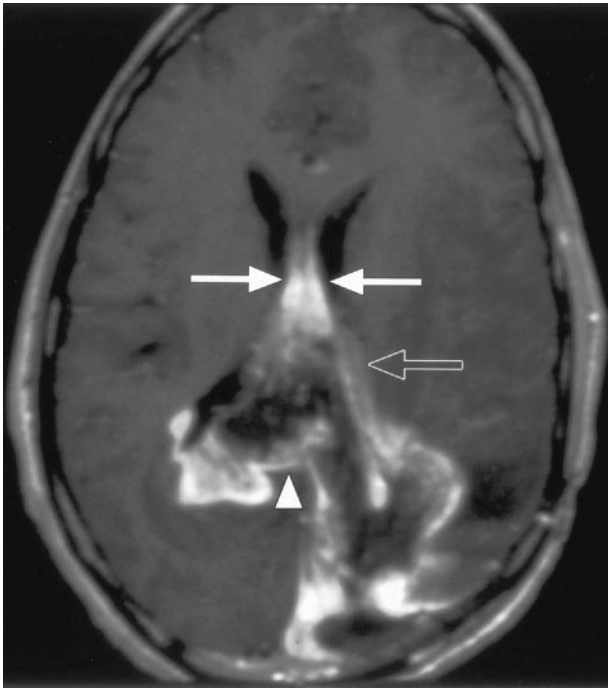
FIG 4.   68-year-old man with history of left parietooccipital glioblastoma multiforme has new abnormal enhancement on follow-up imaging after surgery and proton beam irradiation therapy. Arrows on this postcontrast axial T1-weighted image illustrate enhancement and thickening of the septum pellucidum. Arrowhead points to involvement of the corpus callosum. Open arrow points to subependymal spread. Multiple new lesions were identified. Biopsy of a portion of the corpus callosum abnormality (*arrowhead*) yielded recurrent tumor.

complexity of the neuroradiological diagnosis and hence overestimate the importance of the individual signs. We have attempted to alleviate these potential biases by presenting the implications from the results as guidelines. Radiation doses were not standardized and thus data correlation to the patient dose and timing would be possibly useful, but because of the time of performance of this study and the fact that some of the patients received treatment from other facilities as well, correlation of these data are not available with fidelity. Thus, further study with this type of correlation is also indicated.

Pretreatment imaging revealed T2 hyperintensity with variable, heterogeneous enhancement as is typical for high-grade gliomas. Serial imaging following surgical debulking and proton beam radiation treatment were performed for all patients. Because even initially nonenhancing gliomas may develop enhancement with time, the development of new enhancement, either at or distant from the resection margins, could potentially be attributable to either high-grade recurrence or radiation necrosis.

Finally, it is not our intent to describe these results as support for obviating biopsy or functional imaging but rather to help extract as much data as possible from the conventional MR imaging examinations that patients with high-grade gliomas routinely undergo as a first line both for surveillance and clinical problem-focused evaluation. Our premise was to identify conventional MR

enhancement patterns, in post–proton beam–treated patients with gliomas, which favor either predominantly tumor recurrence or predominantly radiation necrosis. Our goal was not to obviate advanced imaging or biopsy but rather to extract as much data as possible from the conventional MR imaging, so as to better determine the need for these additional studies.

In conclusion, in proton beam–treated patients with gliomas, corpus callosum involvement, in conjunction with multiple enhancing lesions with or without crossing of the midline and subependymal spread, favors predominant glioma progression. Overall, combinations of enhancement patterns were more likely than individual patterns to distinguish necrosis from predominant tumor progression. Thus, our hypothesis that some combinations of conventional MR imaging findings may be clinically useful is thus supported. Together with clinical and functional imaging findings, these results could assist in determining the management of this patient population, including the need for biopsy and/or follow-up examinations.

References

1. Biousse V, Newman NJ, Hunter SB, Hudgins PA. **Diffusion-weighted imaging in radiation necrosis.** *J Neurol Neurosurg Psychiatry* 2003;74:382–384
2. Chan YL, Yeung DK, Leung SF, Chan PN. **Diffusion-weighted magnetic resonance imaging in radiation-induced cerebral necrosis: apparent diffusion coefficient in lesion components.** *J Comput Assist Tomogr* 2003;27:674–680
3. Hein PA, Eskey CJ, Dunn JF, Hug EB. **Diffusion-weighted imaging in the follow-up of treated high-grade gliomas: tumor recurrence versus radiation injury.** *AJNR Am J Neuroradiol* 2004;25:201–209
4. Aksoy FG, Lev MH. **Dynamic contrast-enhanced brain perfusion imaging: technique and clinical applications.** *Semin Ultrasound CT MR* 2000;21:462–477
5. Aronen HJ, Perkio J. **Dynamic susceptibility contrast MRI of gliomas.** *Neuroimaging Clin N Am* 2002;12:501–523
6. Schlemmer HP, Bachert P, Henze M, et al. **Differentiation of radiation necrosis from tumor progression using proton magnetic resonance spectroscopy.** *Neuroradiology* 2002;44:216–222
7. Chao ST, Suh JH, Raja S, Lee SY, Barnett G. **The sensitivity and specificity of FDG PET in distinguishing recurrent brain tumor from radionecrosis in patients treated with stereotactic radiosurgery.** *Int J Cancer* 2001;96:191–197
8. Wong TZ, van der Westhuizen GJ, Coleman RE. **Positron emission tomography imaging of brain tumors.** *Neuroimaging Clin N Am* 2002;12:615–626
9. Henze M, Mohammed A, Schlemmer HP, et al. **PET and SPECT for detection of tumor progression in irradiated low-grade astrocytoma: a receiver-operating-characteristic analysis.** *J Nucl Med* 2004;45:579–586
10. Castel JC, Caille JM. **Imaging of irradiated brain tumours: value of magnetic resonance imaging.** *J Neuroradiol* 1989;16:81–132
11. Kumar AJ, Leeds NE, Fuller GN, et al. **Malignant gliomas: MR imaging spectrum of radiation therapy- and chemotherapy-induced necrosis of the brain after treatment.** *Radiology* 2000;217:377–384
12. Fitzek MM, Thornton AF, Rabinov JD, et al. **Accelerated fractionated proton/photon irradiation to 90 cobalt gray equivalent for glioblastoma multiforme: results of a phase II prospective trial.** *J Neurosurg* 1999;91:251–260
13. Fitzek MM, Thornton AF, Harsh GT, et al. **Dose-escalation with proton/photon irradiation for lower-grade glioma: results of an institutional phase I/II trial.** *Int J Radiat Oncol Biol Phys* 2001;51:131–137
14. Burger PC, Mahley MS Jr, o L, Vogel FS. **The morphologic effects of radiation administered therapeutically for intracranial gliomas: a postmortem study of 25 cases.** *Cancer* 1979;44:1256–1272
15. Marks JE, Baglan RJ, Prassad SC, Blank WF. **Cerebral radionecrosis: incidence and risk in relation to dose, time, fractionation and volume.** *Int J Radiat Oncol Biol Phys* 1981;7:243–252